

Measurement of the *K*-Shell Ionization Cross Sections of Al and Mg for 1- to 5-MeV α Particles*

Bach Sellers, Frederick A. Hanser, and Henry H. Wilson

Panametrics, Incorporated, Waltham, Massachusetts 02154

(Received 3 February 1969)

The *K*-shell ionization cross sections of Al and Mg for 1- to 5-MeV α particles have been obtained from measurements of the fluorescent x-ray yields of thin foils irradiated by α particles. The results for Al range from $(0.36 \pm 0.31) \times 10^{-20}$ cm² at 1.0 MeV to $(13.47 \pm 0.77) \times 10^{-20}$ cm² at 5.0 MeV, and for Mg from $(1.04 \pm 0.25) \times 10^{-20}$ cm² at 1.0 MeV to $(16.61 \pm 0.56) \times 10^{-20}$ cm² at 5.0 MeV. The energy dependence is stronger than predicted by the Born approximation. The data are compared with theoretical calculations and with other experimental results for protons, He³, and α particles.

I. INTRODUCTION

The production of characteristic atomic x rays by heavy, fast-moving charged particles has been a subject for both theoretical and experimental investigation since the work of Chadwick as early as 1913.¹ A theoretical treatment of inner shell ionization was first undertaken by Henneberg² who obtained an approximate formula for the *K*-shell ionization cross section. More recently, Merzbacher and Lewis³ have presented Born approximation calculations for the *K* and *L* shells.

The first detailed measurements of x-ray yields were made by Bothe and Fränz⁴ using 5.3-MeV Po²¹⁰ α particles and absorption foils for x-ray energy determination. With the exception of one measurement for Al, this work used thick (totally absorptive for the particles) targets. Bühring and Haxel⁵ also used Po²¹⁰ α particles to measure absolute thick target yields for several elements. In none of this early work was any attempt made to calculate cross sections from the yield data, although the measurements of Bothe and Fränz⁴ do include a relative yield curve for 2- to 5.3-MeV α particles on Al, which in principle would allow the calculation of an ionization cross section when used in conjunction with their absolute yield measurement at 5.3 MeV. More recently, thick target measurements have been made using protons, He³, and α particles from accelerators^{6,7} and pulse-height analysis for x-ray energy determination. The cross sections have been calculated using a method developed by Merzbacher and Lewis³ involving differentiation of the yield curve. Data for Mg and Al, on which much work has been done, extend from 25 keV to 1.7 MeV for protons,⁶ while He³ and α -particle measurements extend only over the range 30 to 200 keV.⁷

It was decided to extend the range of the recent α -particle measurements on Mg and Al from 1 to 5.5 MeV. The available theoretical treatments would then allow a comparison of proton and α -

particle data for these two elements over a very large energy range.

The experimental method uses a 100- μ Ci Am²⁴¹ source to supply the high-energy α particles. Foils are used for energy variation, a solid-state detector for α -particle energy measurement, and a flow proportional counter for detection of the fluorescent x rays. Our method differs from that of previous investigators in that the bulk of our measurements were made with foils thin enough that the α particles do not deposit all of their energy in the foil. Both the incident and exit energies could be measured, allowing a direct determination of the stopping power values used in the data analysis. A method of calculating the cross section is utilized, that is different from that used for thick targets. Particularly at high energies, where fractional energy losses in the foil are small, more accurate cross sections should be obtainable with this method. Our yield measurements give a value for 5-MeV α particles incident on Al which is several times the result of Bothe and Fränz.⁴

II. EXPERIMENTAL METHOD

A. Apparatus and Procedure

The experimental layout is shown in Fig. 1. A thin foil of Al or Mg is supported in a vacuum chamber and irradiated with α particles from a 100- μ Ci vacuum-sublimed Am²⁴¹ source. A solid-state detector, with a covering grid to reduce the count rate to manageable limits, is used to measure the energy and flux of the α particles both incident on and penetrating the foil. The fluorescent x rays from the target foil are detected by a flow proportional counter with a 0.875-in. diam \times 0.25-mil thick Mylar window supported by a screen grid with 65% transmission.

The energy of the α particles is varied by placing layers of 0.15-mil Mylar foils over the Am²⁴¹ source and by changing the air path of the α par-

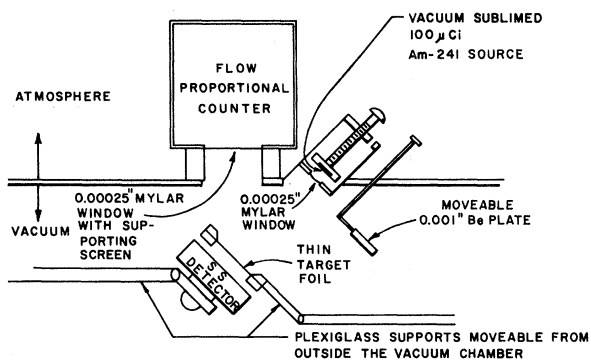


FIG. 1. Experimental layout for measuring α -particle-excited x-ray cross sections. Some of the higher-energy α -particle data were taken with the Am^{241} source in the vacuum chamber.

ticles. For energies above 4 MeV, the Am^{241} source was mounted in the vacuum chamber and only the Mylar foils were used for energy variation.

The flow proportional counter was operated with P -10 gas (90% argon plus 10% methane) at one atmosphere. The relative detection efficiency of the proportional counter for the 1.49-keV Al K x rays was measured at several gas pressures and reached a plateau, showing that for one atmosphere of P -10 gas the detection efficiency for Al (and the 1.25-keV Mg) K x rays is equal to the window transmission, with essentially all transmitted x rays being absorbed in the gas. For gas pressures up to one atmosphere, no decrease was observed in relative detection efficiency because of x-ray absorption too near the entrance window. The transmission of the 0.25-mil Mylar window and screen support was measured to be 0.288 for the 1.49-keV Al K x ray, and 0.177 for the 1.25-keV Mg K x ray.

The foil targets were mounted on a Plexiglas support which was movable from outside the vacuum chamber. This allowed either the target or a Plexiglas ring shaped like the target holder to be positioned in front of the proportional counter and α source. With this arrangement the solid-state detector could measure the energy of the α particles either before entering or after passing through the target foil. The target foils had an irradiated area of 2.5-cm diam and were either 1.029 mg/cm² of Al or 1.24 mg/cm² of Mg. The α particles entered the foils normally while the fluorescent x rays left at an average angle of 42.5° to the normal. The foils were situated about 5.1 cm from the proportional-counter window.

The solid-state detector was a 4.50-cm² silicon-surface barrier detector with a 200- μ depletion depth, and was covered with a grid which was 9.4% open. The detector was movable from outside the

vacuum chamber which allowed it to be positioned in front of a weak calibration Am^{241} α source mounted inside the vacuum chamber. During x-ray spectrum measurements with the proportional counter the solid-state detector was placed out of the view of the proportional counter to avoid any interference by silicon x rays produced by α particles striking the solid-state detector.

Since the Am^{241} source emits several γ rays as well as neptunium L - and M -shell x rays, provision was made to ensure that the measured Al and Mg x-ray yields arose from α particle as opposed to photon excitation. This was done by means of a movable 1-mil Be disk 1.25 cm in diameter. The target-foil x-ray spectrum was measured first with the α source uncovered, and then had background subtracted while the α source was covered with the Be disk. Since the Be disk transmits over 80% of all x rays above 2.5 keV and stops all α particles below 5 MeV, this background in the K x ray yield arose principally from photon absorption.

A typical measured Al x-ray spectrum is shown in Fig. 2. The plots are 4-channel sums of the pulse-height spectrum of the flow counter taken with a 128-channel analyzer, the upper being the

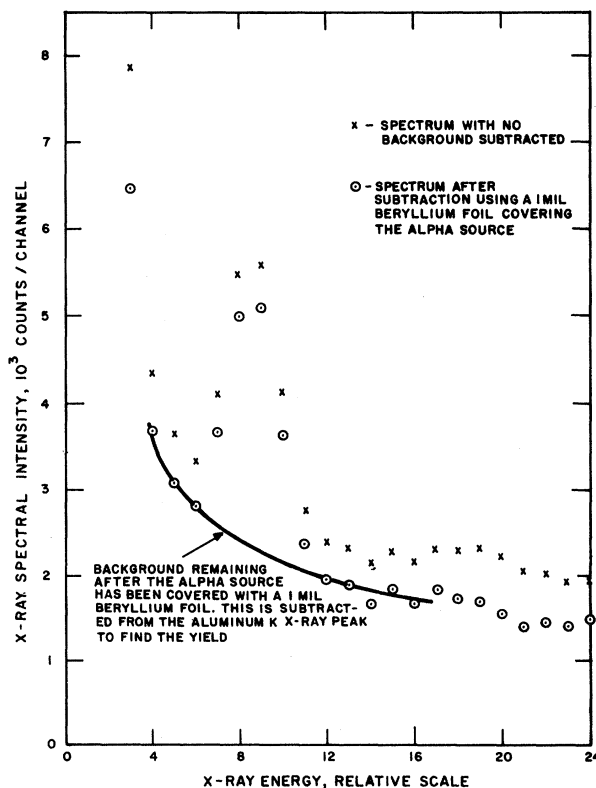


FIG. 2. A typical measured Al x-ray spectrum taken with the flow proportional counter.

measured spectrum with α particles irradiating the foil, while the lower is the result of the upper after subtraction of the background remaining when the α source is covered by the 1-mil Be disk. Also shown is the background curve used to obtain the fluorescent x-ray yield. This background curve was verified by measurements using a 0.3-mil Mylar target.

B. Data Analysis

There are three stages in the analysis of data. First, the experimental measurements must be utilized to determine yields, in terms of fluorescent x rays/(sr α particle), and the associated statistical errors. Second, it must be shown that the fluorescent x rays are not produced by x rays from the Am^{241} source but, within statistical errors, arise from α -particle interactions. Finally, the yields must be converted into ionization cross sections for the K shell.

The yields and errors were calculated in the following manner. Smooth background curves were drawn on the measured x-ray spectra, as shown in Fig. 2, and then subtracted from the counts summed over the peak. The error in the counts summed over the peak arises from counting statistics, and is just the square root of the total number of counts entering the calculations (note that one type of background has already been subtracted and thus influences this error). In general, about 3 points above and 3 points below the x-ray peak were used to find the remaining background. The error in this background was taken to be the statistical error in a straight-line fit to the background, although the actual subtraction used a rounded curve. The result is a K x-ray intensity N_x (x-rays/sec) and an associated error (standard deviation). The α -particle intensity N_α (α particles/sec) striking the target foil was taken from the solid-state detector measurements with the foil in place, except for the lowest-energy α particles which did not penetrate the foil. It was found that errors in repositioning the target foil and solid-state detector led to variations of a few percent in the measured α -particle intensity, so the error in the incident α -particle intensity was taken to be 5%. Similarly, the error in the product of detection efficiency ϵ of the proportional counter and its solid angle Ω as seen from the target foil was taken to be 5%. The errors in N_x , N_α , and $\epsilon\Omega$ were combined on an rms basis to obtain the total error, and the yield was calculated from

$$Y = N_x / (N_\alpha \epsilon \Omega) \text{ x rays/(sr } \alpha), \quad (1)$$

where $\epsilon = 0.288$ for Al and 0.177 for Mg K x rays, and $\Omega = 0.150$ sr.

Arguments that the measured yields are not af-

ected by the Am^{241} x-ray background can be made on two lines. The subtraction of background when the Am^{241} source is covered with 1 mil of Be should subtract a substantial amount of any x-ray-produced fluorescent x rays. To excite a K x ray, the incident x-ray energy must be above the corresponding K edge, 1.56 keV for Al and 1.30 keV for Mg. The transmission of 1 mil of Be at these energies is 0.45 and 0.26, respectively. Thus for Al a minimum of about half of the x-ray produced K x rays would be subtracted, since higher-energy x rays are even less attenuated than at 1.56 keV. In practice, no statistically significant differences were found for the Al yields before and after the run with the Be disk over the source. For the Mg target a minimum of 26% of the x-ray produced K x rays would be subtracted, and again no statistically significant differences were found.

Another approach is to use the measured x-ray intensities emitted by Am^{241} and calculate the expected K x-ray yields. The Am^{241} photon spectrum and relative intensities per α particle were measured by Magnusson,⁸ and while the 3.3-keV Np M x ray intensity was not listed, a rough value of 0.07 x rays per α particle can be calculated from a spectrum shown by Magnusson and by data given for his detector. Measurements for our source indicate a relative intensity near 10^{-2} x rays per α particle although in the calculations we use the higher value obtained by Magnusson. The mass-absorption coefficients of Al and Mg for the 3.3-keV x rays as well as for their own fluorescent K x rays were obtained from interpolations of averages of values listed in data compilations by Stainer,⁹ and by Henke *et al.*,¹⁰ and the K -shell fluorescent yields for Al (0.0377) and Mg (0.0277) were calculated from a formula of Bailey and Swedlund¹¹ which they found to be most accurate near $Z = 13$, Al. Using this method we find that the total K x-ray yield arising from the 3.3-keV x rays is negligible compared with the errors in the measured yield, especially after subtraction of the x-ray spectrum remaining when the Am^{241} source is covered with the 1-mil Be disk. Higher energy x rays from Am^{241} contribute even less and there is no appreciable x-ray intensity from Am^{241} in the range 1 to 3 keV. Thus the Am^{241} x-ray contribution to the measured fluorescent x-ray yields is negligible, in agreement with the experimental findings.

The K -shell ionization cross sections $\sigma_K[E_\alpha]$ were obtained from the yields as follows. The yield can be written as

$$Y = (n\omega_K/4\pi) \int_0^t \sigma_K[E_\alpha(t)] \times \exp[-(\mu/\rho)_K t \sec\theta_x] dt, \quad (2)$$

where $n = N_0/M$, with N_0 Avogadro's number, M

the atomic weight of the target, ω_K the K -shell fluorescent yield of the target material, $(\mu/\rho)_K$ the K x-ray absorption coefficient of the target material in cm^2/g , t the target thickness in g/cm^2 , and θ_x the angle of the K x-ray emission to the target foil normal. $E_\alpha(t)$ is the average energy of the α particles at the depth t in the target foil, and depends on the incident particle energy. The experimental yields were measured for incident α energies of roughly 1 to 5.5 MeV in 0.5 MeV steps. Since the α particles lost about 1 MeV in the foil, two consecutive energy measurements involved a total α -particle energy range of about 1.5 MeV. From the discussion in Ref. 3, it was felt that a power law form

$$\sigma_K[E_\alpha(t)] = \sigma_0 E_\alpha(t)^a, \quad (3)$$

where σ_0 and a are adjustable parameters, could be used to approximate the K -shell ionization cross section for the purposes of data analysis. This would allow σ_0 and a to be determined from two consecutive energy yield measurements. For this purpose a short computer program was written to integrate (2) using (3). The program adjusted σ_0 and a until a fit to the two yields was obtained. A cross section $\sigma_K(\bar{E}_\alpha)$ was then calculated using an energy \bar{E}_α slightly higher than the average α -particle energy for the two yields in question. \bar{E}_α was generally chosen as a multiple of 0.5 MeV. The error in $\sigma_K(\bar{E}_\alpha)$ was calculated from the errors in the yields by a straightforward error analysis assuming Gaussian distributions, the necessary partial derivatives being calculated numerically from the output of the fitting program. All errors given are standard deviations from an assumed Gaussian distribution.

A comment should be made about the range-energy relations used to calculate $E_\alpha(t)$. The α -particle ranges in Al were obtained from the tabulation in Whaling¹² for energies above 3 MeV, and from integration downward from 3 to 0.6 MeV using his listed stopping cross sections. The results were fitted with the form

$$R = R_0(E_\alpha + \epsilon_0)^b \quad (4)$$

with $R_0 = 0.01983$, $\epsilon_0 = 5.13$ MeV, and $b = 2.52$ yielding R in mg/cm^2 . The relation (4) was found to fit the data of Whaling to 1.5% over the range 0.6 to 6 MeV, and made calculation of $E_\alpha(t)$ somewhat simpler during data analysis. For Mg, the proton stopping-power calculations of Janni¹³ were converted to α -particle stopping powers at $E_\alpha = 3.97E_p$ using the average ratios given by Whaling, for α particles of less than 2 MeV. For α particles above 2 MeV the calculations of Hill *et al.*¹⁴ were used. Here it was found that (4) with $R_0 = 0.05460$, $\epsilon_0 = 3.67$ MeV, and $b = 2.20$ gave a fit

to 1% over the range 0.8 to 6 MeV, and to 3% down to 0.6 MeV. Since entrance and exit α energies were measured, the relation (4) was also checked experimentally and found to hold to 3% for Al and to 4% for Mg, to an exit energy of 1 MeV.

Our final consideration is the effect of the finite spread of the α -particle energy distribution. Since foils were used to reduce the Am^{241} α -particle energy, the lower-energy data were obtained with an incident beam of several percent resolution full width at half maximum. If we approximate these distributions by Gaussian forms with an average energy of \bar{E}_α and a standard deviation of σ_α , then the strong energy dependence of $\sigma_K(\propto E_\alpha^4)$ will increase the yield slightly over what would be observed with a monoenergetic beam of energy $\bar{E}_\alpha + \delta E_\alpha$. Approximate calculations show that δE_α is generally on the order of a few keV, with a maximum of about 30 keV for $\bar{E}_\alpha \approx 1$ MeV. These errors can be neglected when compared with the statistical errors in the yields.

III. RESULTS

A. Aluminum

The experimental x-ray yields for Al are listed in Table I. Some of the yields are averages of two or more sets of data. For each yield the measured entrance and exit energies of the α particles are listed, as well as the calculated exit energy using the incident energy, the foil thickness, and Eq. (4) for the range-energy relation. The agreement of the experimental and calculated exit energies to 3% over the range 5 to 1 MeV shows that

TABLE I. Experimental aluminum K x-ray yields from α -particle bombardment. Foil thickness = 1.029 mg/cm^2 ; $(\mu/\rho)_K = 405$ cm^2/g (selected average from Refs. 9 and 10).

α energy (MeV)			Experimental yield [10^{-3} x-rays/(sr α)]
Measured In	Measured Out	Calculated ^a Out	
1.19	•••	•••	0.079 \pm 0.068
1.65	0.45	0.31	0.482 \pm 0.154
2.14	0.97	0.97	0.91 \pm 0.12
2.76	1.79	1.75	1.89 \pm 0.13
2.98	2.07	2.02	2.73 \pm 0.14
3.47	2.61	2.60	2.90 \pm 0.19
3.97	3.20	3.19	4.56 \pm 0.27
4.49	3.77	3.78	6.34 \pm 0.48
5.01	4.36	4.36	6.95 \pm 0.54
5.45	4.84	4.84	7.19 \pm 0.57

^aCalculated from Eq. (4) with the parameters given for aluminum, using the measured incident energy and foil thickness.

when compared with the experimental yields which have a minimum error of 6%, Eq. (4) is sufficiently accurate for use in calculating the cross sections. The lowest two energy yields have errors of 32 and 86%, and thus the increased error in (4) below 1 MeV should still not contribute significantly to the error in the cross sections.

Table II lists the experimental fluorescent x-ray production cross sections and the K -shell ionization cross sections of Al by α particles. These results were obtained from the yields in Table I using the method of analysis described earlier. The errors are standard deviations in an approximate Gaussian distribution. The fluorescent x-ray production cross section is what is measured directly while the ionization cross section is obtained by division by the K -shell fluorescent yield, ω_K . Figure 3 is a plot of the data in Table II in terms of $Z_K^4 \sigma_K / z^2$ versus η_K [see Eq. (5)], along with the proton data of Khan *et al.*,⁶ and the proton, α particle, and He³ data of Brandt *et al.*⁷ The data from these two references have been corrected to a K -shell fluorescence yield of $\omega_K = 0.0377$.

B. Magnesium

The experimental x-ray yields for magnesium are listed in Table III which has the same format as Table I. Table IV lists the resulting fluorescent x-ray production cross sections and the K -shell ionization cross sections of magnesium by α particles. Figure 4 is a plot of the data in Table IV. The data from Refs. 6 and 7 have been corrected to a K -shell fluorescence yield of $\omega_K = 0.0277$.

IV. DISCUSSION

Merzbacher and Lewis³ give the Born approximation K -shell ionization cross section in graph-

TABLE II. Cross section for fluorescent x-ray production and for K -shell ionization of aluminum by α particles; $\omega_K = 0.0377$.

α energy (MeV)	Fluorescent x-ray cross section (10^{-21} cm ²)	K -shell ionization cross section (10^{-20} cm ²)
1.0	0.134 ± 0.115	0.36 ± 0.31
1.5	0.591 ± 0.082	1.57 ± 0.22
2.0	0.963 ± 0.074	2.55 ± 0.20
2.5	1.52 ± 0.071	4.03 ± 0.19
3.0	1.99 ± 0.105	5.28 ± 0.28
3.5	2.93 ± 0.134	7.77 ± 0.36
4.0	4.10 ± 0.22	10.88 ± 0.58
4.5	4.81 ± 0.27	12.76 ± 0.72
5.0	5.08 ± 0.29	13.47 ± 0.77

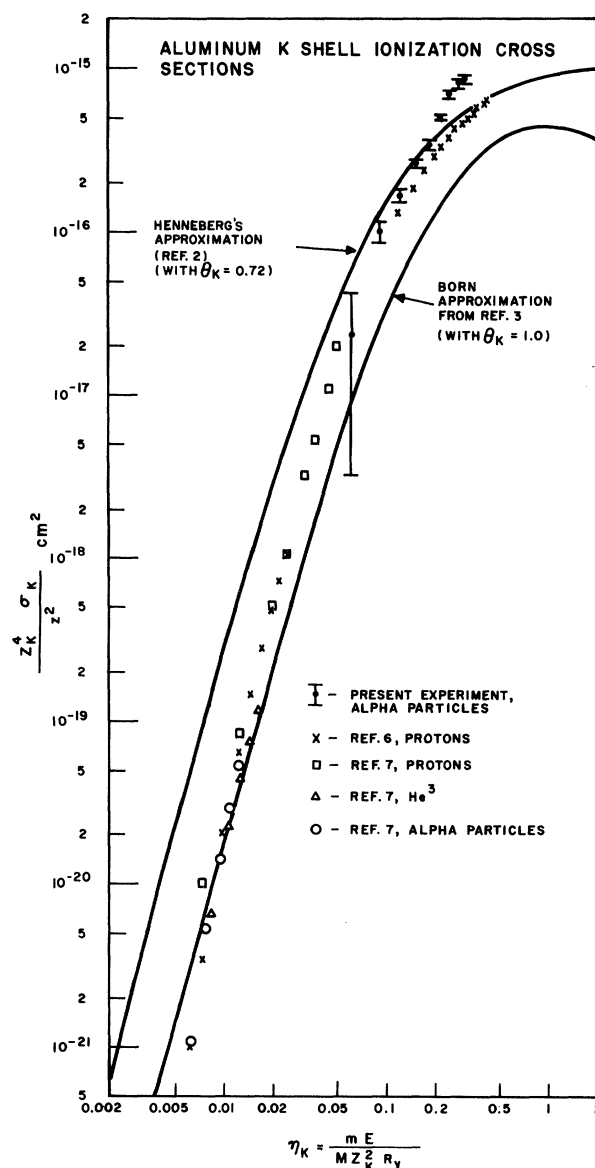


FIG. 3. Plot of the measured Al K -shell ionization cross sections of a number of investigators, comparing them with some theoretical cross sections.

ical form as $Z_K^4 \sigma_K / z^2$ versus η_K where $Z_K = Z - 0.3$, ze is the charge of the incident particles, and

$$\eta_K = mE / MZ_K^2 Ry, \quad (5)$$

where m is the electron mass, M and E are the mass and energy of the incident particles, and Ry is the Rydberg constant = 13.60 eV. The graph is for a K -shell shielding factor of $\theta_K = 1.0$, whereas better values are $\theta_K = 0.72$ for Al and $\theta_K = 0.71$ for Mg. The cross sections can also be calculated from an approximation by Henneberg (Ref. 2, but

TABLE III. Experimental magnesium K x-ray yields from α -particle bombardment. Foil thickness = 1.24 mg/cm²; $(\mu/\rho)_K = 480$ cm²/g (selected average from Refs. 9 and 10).

α energy (MeV)		Experimental yield [10 ⁻³ x rays/(sr α)]
Measured In	Calculated ^a Out	
1.14	...	0.152 \pm 0.080
1.74	...	0.473 \pm 0.068
2.51	1.14	2.08 \pm 0.24
3.00	1.82	2.93 \pm 0.15
3.58	2.53	4.38 \pm 0.35
4.00	3.00	5.55 \pm 0.42
4.47	3.59	6.04 \pm 0.21
5.02	4.22	7.13 \pm 0.40
5.44	4.67	7.93 \pm 0.32

^aCalculated from Eq. (4) with the parameters given for magnesium, using the measured incident energy and foil thickness.

TABLE IV. Cross sections for fluorescent x-ray production and for K-shell ionization of magnesium by α particles; $\omega_K = 0.0277$.

α energy (MeV)	Fluorescent x-ray cross section (10 ⁻²¹ cm ²)	K-shell ionization cross section (10 ⁻²⁰ cm ²)
1.0	0.228 \pm 0.068	1.04 \pm 0.25
1.5	0.500 \pm 0.062	1.81 \pm 0.22
2.5	1.73 \pm 0.081	6.25 \pm 0.29
3.0	2.39 \pm 0.143	8.63 \pm 0.52
3.5	3.15 \pm 0.188	11.37 \pm 0.63
4.0	3.55 \pm 0.115	12.82 \pm 0.42
4.5	4.05 \pm 0.164	14.62 \pm 0.59
5.0	4.60 \pm 0.154	16.61 \pm 0.56

also given in Ref. 3) which allows calculations to be made easily for any value of θ_K .

The experimental K-shell ionization cross sections are most conveniently plotted as $Z_K^4 \sigma_K / z^2$ versus η_K , since this allows comparison of the results for different incident particles. Except for variations in θ_K , this form of graph also allows comparison of the results for different elements. Figures 3 and 4 are such plots of the present results as well as those of other investigators.^{6,7} The two curves are the Born approximation from Ref. 3, with $\theta_K = 1.0$, and Henneberg's approximation² using $\theta_K = 0.72$ for Al and $\theta_K = 0.71$ for Mg.

The data in Figs. 3 and 4 show the same general trends. The results from protons, He³, and α particles show general agreement for values of η_K less than 0.1. For values of η_K less than 0.05, the data can be fitted by a power law,

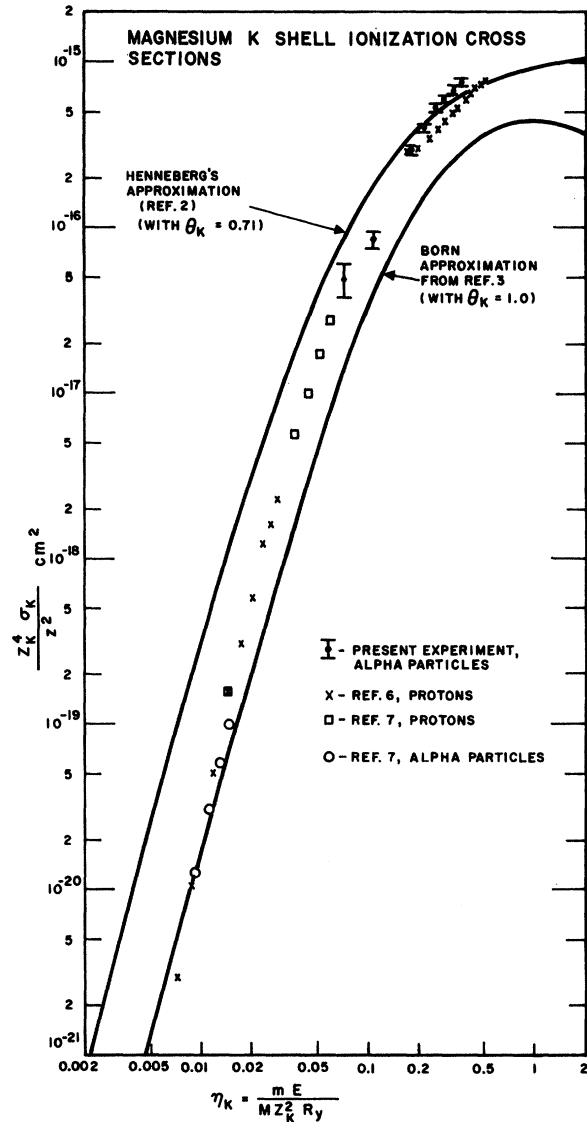


FIG. 4. Plot of the measured Mg K-shell ionization cross sections of a number of investigators, comparing them with some theoretical cross sections.

$$Z_K^4 \sigma_K / z^2 \propto \eta_K^{4.5} \quad (6)$$

which is a slightly stronger energy dependence than theory ($\propto \eta_K^4$ at low energies). Above $\eta_K = 0.1$, the α -particle data become increasingly greater than the proton data.

The above results can be qualitatively explained as a breakdown of the Born approximation. At low energies the wave function of the incident particle is significantly distorted by the target nucleus, while at high energies the incident particle distorts the electron orbits.¹⁵ The latter factor is more severe for α particles than for protons, as is borne out by the data, which show such de-

viations in the region $\eta_K \approx 0.1$ to 0.3.

Bothe and Fränzl⁴ measured the absolute K x-ray yield of Al for 5.3 MeV Po^{210} α particles. They used an ionization chamber to measure ion pair production, and attenuation by foils to separate the soft Al K x ray from harder background. Their result was 56 K x rays per 1000 α particles for Al, with relative measurements then giving 54 x rays per 1000 α particles for Mg. The results listed in Tables I and III can be converted to approximate total yields. If several different energy yields are added to give the yield for the entire path length, the results multiplied by 1.3 to take approximate account of the partial attenuation of the x rays by the target foil and then multiplied by 4π to give the total yield, we obtain 340 x rays per 1000 α particles for Al and 280 x rays per

1000 α particles for Mg. These results are several times larger than those of Bothe and Fränzl. The discrepancy can be partially accounted for by the Al x-ray attenuation coefficient used by Bothe and Fränzl, which was 349 cm^2/g . Correction to 404 cm^2/g accounts for roughly a factor of 2. The remaining discrepancy is presently unexplained.

By differentiation of the yield curve Bothe and Fränzl also measured the relative x-ray yield per unit path length in air for Al. Using the α -particle energy-loss tables of Ref. 14 for air and Al, their results can be converted into a relative K -shell ionization cross section as a function of α -particle energy. If these relative cross sections are then normalized to our data, they show good agreement on the variation of the ionization cross section with energy.

*Sponsored in part by the Division of Isotopes Development of the U. S. Atomic Energy Commission Contract No. AT(30-1)-3491, and by Panametrics, Inc. (see U. S. Patent 3, 408, 496, October, 1968).

¹J. Chadwick, *Phil. Mag.* **25**, 193 (1913); **24**, 594 (1912).

²W. Henneberg, *Z. Physik* **86**, 592 (1933).

³E. Merzbacher and H. W. Lewis, in *Handbuch der Physik*, edited by S. Flügge (Springer-Verlag, Berlin, 1958), Vol. 34, pp. 166-192. See also H. W. Lewis, B. E. Simmons, and E. Merzbacher, *Phys. Rev.* **91**, 943 (1953).

⁴W. Bothe and H. Fränzl, *Z. Physik* **52**, 466 (1929).

⁵W. Böhning and O. Haxel, *Z. Physik* **148**, 653 (1957).

⁶J. M. Khan, D. L. Potter, and R. D. Worley, *Phys. Rev.* **139**, A1735 (1965); earlier work is described in *Phys. Rev.* **133**, A890 (1964); **134**, A316 (1964); **135**, A511 (1964); **136**, A108 (1964).

⁷W. Brandt, R. Laubert, and I. Sellin, *Phys. Rev.* **151**, 56 (1966).

⁸L. B. Magnusson, *Phys. Rev.* **107**, 161 (1957).

⁹H. M. Stainer, *X-Ray Mass Absorption Coefficients*, United States Bureau of Mines, Information Circular No. IC-8166, 1963 (unpublished).

¹⁰B. L. Henke, R. L. Elgin, R. E. Lent, and R. B. Ledingham, U. S. Air Force Office of Scientific Research Report No. AFOSR 67-1254, 1967 (unpublished).

¹¹L. E. Bailey and J. B. Swedlund, *Phys. Rev.* **158**, 6 (1967).

¹²W. Whaling, in *Handbuch der Physik*, edited by S. Flügge (Springer-Verlag, Berlin, 1958), Vol. 34, pp. 193-217.

¹³J. F. Janni, Air Force Weapons Laboratory Technical Report No. AFWL-TR-65-150, Kirtland Air Force Base, New Mexico, 1966 (unpublished).

¹⁴C. W. Hill, W. B. Ritchie, and K. M. Simpson, Report Nos. ER-7777 (Lockheed-Georgia Company) and NASA CR-69434 (unpublished), Vol. I.

¹⁵Reference 5, p. 184.